ELSEVIER

Forecasting giant, catastrophic slope collapse: lessons from Vajont, Northern Italy

Christopher R.J. Kilburn [a,*], David N. Petley [b]

[a] Benfield Greig Hazard Research Centre, Department of Earth Sciences, University College London, Gower Street, London WC1E 6BT, UK
[b] Department of Geography, Science Laboratories, University of Durham, Durham DH1 3LE, UK

Abstract

Rapid, giant landslides, or sturzstroms, are among the most powerful natural hazards on Earth. They have minimum volumes of $\sim 10^6 - 10^7$ m^3 and, normally preceded by prolonged intervals of accelerating creep, are produced by catastrophic and deep-seated slope collapse (loads $\sim 1 - 10$ MPa). Conventional analyses attribute rapid collapse to unusual mechanisms, such as the vaporization of ground water during sliding. Here, catastrophic collapse is related to self-accelerating rock fracture, common in crustal rocks at loads $\sim 1 - 10$ MPa and readily catalysed by circulating fluids. Fracturing produces an abrupt drop in resisting stress. Measured stress drops in crustal rock account for minimum sturzstrom volumes and rapid collapse accelerations. Fracturing also provides a physical basis for quantitatively forecasting catastrophic slope failure.
© 2003 Elsevier Science B.V. All rights reserved.

1. Introduction

Sturzstroms are giant landslides of shattered rock that collapse with accelerations of some $0.5 - 1$ m s^{-2} and can travel kilometres within minutes (Hsü, 1975). They are triggered by catastrophic slope failure in all regions of high relief, from young mountain chains to volcanic edifices, and on Earth, involves volumes from $\sim 10^6 - 10^7$ m^3 to $\sim 10 - 100$ km^3 (Hsü, 1975; Melosh, 1987). Occurring at least twice a decade, sturzstroms are unstoppable by current defensive techniques, so that evacuation remains the only viable procedure for protecting vulnerable communities. Evacuation alerts, in turn, require a reliable method for forecasting slope failure.

Apart from a few examples triggered by large earthquakes, commonly with Richter Magnitudes greater than 6.5 (Hadley, 1978; McSaveney, 1978; Plafker and Ericksen, 1978; Blodgett et al., 1998), catastrophic slope failure is normally preceded by weeks to decades or more of accelerating creep (Voight, 1978). Failure often appears to occur without warning only because earlier movements have passed unnoticed. Indeed, few data are available for investigating trends in precollapse accelerations. A classic exception is the set of observations compiled for the Alpine Mt. Toc, in which after nearly 3 years of intermittent, slow deformation, collapsed catastrophi-

* Corresponding author.
E-mail address: c.kilburn@ucl.ac.uk (C.R.J. Kilburn).

cally into Italy's Vajont reservoir on 9 October 1963, claiming more than 2000 lives (Müller, 1964).

The collapse of Mt. Toc appears to have been quite ordinary when compared with accounts of other catastrophic slope failures (Ter-Stepanian, 1966; Voight, 1978). These other failures have occurred within a wide range of environments, possibly including lunar and Martian conditions (Howard, 1973; Lopes et al., 1982). Thus, although different processes might induce slope instability, the subsequent approach to catastrophic failure must be determined by a mechanism that can operate independently from local environmental controls. For example, in the case of Mt. Toc, it is generally accepted that raised water pore pressure is crucial to the onset of slope instability (Hendron and Patton, 1985). However, this condition alone cannot account for the accelerating creep before collapse.

Because catastrophic collapses are deep-seated, they normally require the failure of coherent bedrock, and for typical crustal conditions, such failure is invariably brittle. It is plausible, therefore, that rock cracking is the mechanism controlling the acceleration to giant and catastrophic slope failure. As well as being a general failure mechanism, slow rock cracking also happens to be readily catalysed by circulating water (Atkinson, 1984), and so in addition to raised pore pressure, it is attractive as a reason for why slopes should tend to fail when they are wet. Using the Mt. Toc collapse as a case study, this paper applies a new model of slow cracking to describe quantitatively the observed increases in slope movement before collapse. It also shows that slow cracking, as a general mechanism, can account for rapid slope accelerations during collapse and for the threshold volumes that must be exceeded for giant, catastrophic events to occur.

2. The Vajont landslide

The Vajont valley is situated in the dolomite region of the Italian Alps, about 100 km north of Venice. The valley has a broad and deep, glacial morphology, but a very narrow valley mouth. As such, it was identified during Italy's postwar reconstruction as a potential site for a hydroelectric power station. Excavation of the site was initiated in 1956. Four years later, the

dam had been completed. Rising 261.6 m above the valley floor, it was the highest doubly curved arch dam in the world, and it was designed to impound some 150 million m^3 of water. The following summary of events is based on the comprehensive accounts by Müller (1964) and Hendron and Patton (1985).

Soon after dam construction had begun, the geological structure of the Vajont valley aroused concern about the possibility for devastating landslides. Created by glacial and fluvial downcutting through an asymmetric syncline, the valley is flanked by middle Jurassic limestone and overlain by upper Jurassic limestone with clay and Cretaceous limestones (Fig. 1). Dipping into the valley, these formations provided conditions suitable for dip-slope failures. Nevertheless, the designers of the dam concluded that deep-seated landslides were extremely unlikely to occur because (a) test bore holes showed no evidence of weak layers at depth, (b) the asymmetric form of the syncline was expected to act as a natural break on slope movement and (c) seismic surveys suggested that the valley walls consisted of very firm, in situ rock with a high modulus of elasticity.

Filling of the reservoir began in February 1960. By October, when the depth of the reservoir had reached 170 m, joints opened as an M-shaped crack almost 2 km long across Mt. Toc at 500–600 m above the valley floor (Fig. 2). On 4 November, with the depth of the reservoir at 180 m, some 700,000 m^3 of material slid in about 10 min from the toe of the moving mass into the lake.

Attempts were made to stabilise the landslide by inducing movement of the mass until it reached a new condition of stability. Since movement had occurred during filling of the reservoir, it was inferred that raised water pore pressure in the flanks of Mt. Toc was the key destabilising factor. Accordingly, it was assumed that additional movement at a controlled, slow rate could be initiated by elevating the level of the reservoir in a careful manner. Similarly, it was assumed that movement could be halted by lowering the reservoir's level. The strategy appeared to have been successful until mid-1963 when, between April and May, the depth of the reservoir was rapidly increased from about 195 to 230 m. Rates of slope movement increased slightly but never exceeded 0.3 cm day^{-1}. By mid-July, the depth had reached 240 m,
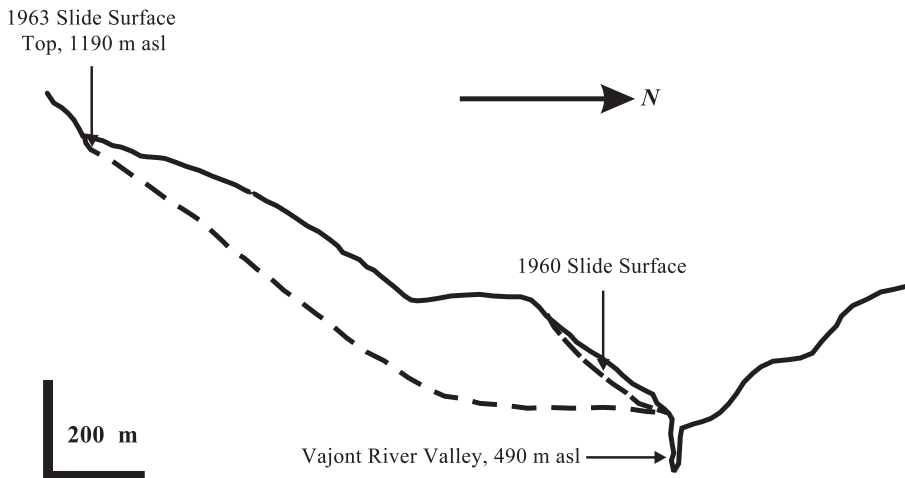
Fig. 1. Cross-section through the western end (near the Vajont dam) of Mt. Toc before catastrophic collapse. The clay-rich layers in which deformation was concentrated occurred in a zone about 1-m thick along the 1963 failure surface. After Semenza and Sapigni (1986), also reproduced in Hendron and Patton (1985) and Semenza and Melidoro (1992).
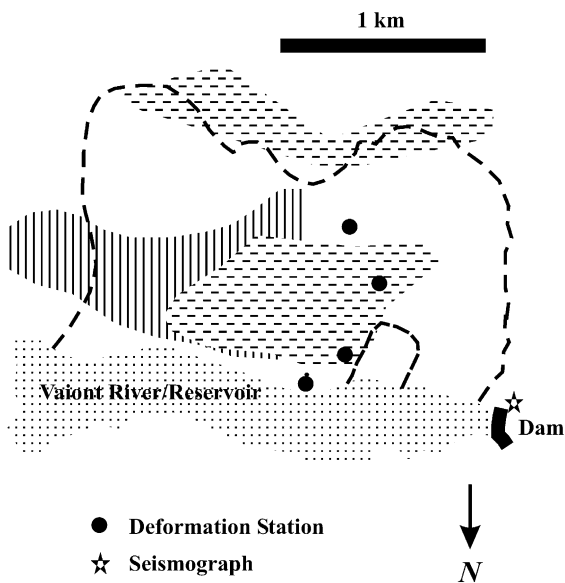

Fig. 2. The Vajont landslide failed along an M-shaped scar (larger dashed line). The preferred location of seismicity recorded across the unstable mass moved from the eastern half in 1960 (vertical shading) to the centre and southern limit in 1962 (dashed shading). The deformation stations shown are the four used in published graphs of Mt. Toc's rate of movement with time. The 1960 collapse (smaller dashed line) was a minor event compared with the 1963 collapse. Data from Belloni and Stefani (1992), Melidoro (1992) and Hendron and Patton (1985).

and some of the control points indicated small increases in displacement to 0.5 cm day^{-1}. Although the same depth was maintained until mid-August, the slope velocity increased to 0.8 cm day^{-1}. By early September, the depth of water was 245 m, by which time the slide velocity had accelerated to 3.5 cm day^{-1} (Fig. 3). With hindsight, this increase to values greater by an order of magnitude than those typical before mid-1963 can be viewed as the first clear signal that, after 3 years of movement, Mt. Toc had entered a more dangerous phase of instability.

In late September, the water level was slowly dropped in an attempt to reduce the rates of movement, and by 9 October, the reservoir's depth had been reduced to 235 m. Even so, slope movements continued to accelerate to more than 20 cm day^{-1}. At 22.39 local time on 9 October, the mountainside collapsed. Some 270 million m^3 of rock slid nearly 500 m northwards at up to 30 m s^{-1}. Blocking the gorge to depths of as much as 400 m, the landslide traveled to 140 m up the opposite bank. The whole event lasted for less than 45 s. At that time, the reservoir contained 115 million m^3 of water. Having washed back and forth along both sides of the valley, a wave of water overtopped the dam by as much as 245 m before crashing onto the villages of Longarone, Pirago, Villanova, Rivalta and Fae. Within minutes,
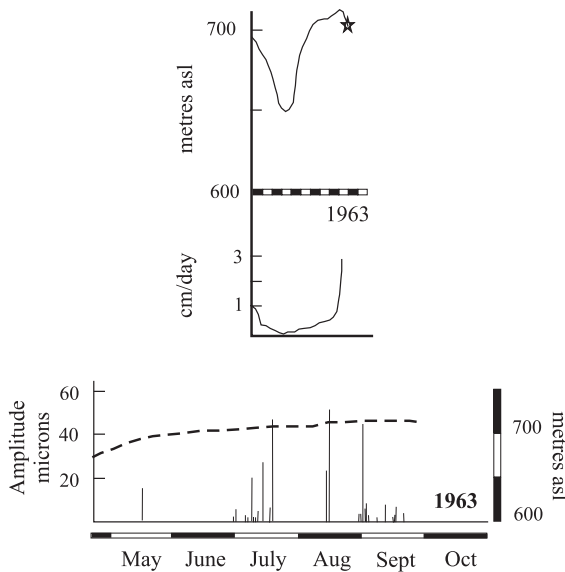
Fig. 3. Changes in rates of horizontal slope movement, seismicity and reservoir level before the catastrophic 1963 collapse of Mt. Toc. Top: rates of slope movement (lower) accelerated to collapse (star) despite late drainage of the reservoir (upper) in October. Velocity measurements averaged from data were obtained from stations near the toe of the moving mass (Fig. 2). Horizontal scale bar in months is from January. After Hendron and Patton (1985). Bottom: seismicity recorded (left scale) from May to September. The dashed line shows the level of water in the reservoir (right scale). After Belloni and Stefani (1992).

about 2000 lives had been lost and the villages swept from view. Incredibly, the Vajont dam remained intact.

3. Investigations of the failure

The tragedy at Vajont has spurred numerous investigations into the conditions triggering slope collapse, including those of Müller (1964), Semenza (1965), Bassett (1978), Voight and Faust (1982), Hendron and Patton (1985), Mantovani et al. (1991) and Semenza and Melidoro (1992). It is now widely agreed that failure occurred along bands of clay within the limestone mass, at depths between 100 and 200 m below the surface (Hendron and Patton, 1985). These clay beds, 5–15 cm thick, represented planes of weakness, which, though subhorizontal at distances less than 400 m from the gorge, were farther away inclined at about 35° into the valley. Raising the level of the lake

increased water pore pressure in the flanks of Mt. Toc, inducing a decrease in effective normal stress and favouring mobilisation of the clay layers. Persistent rainfall shortly before catastrophic failure may also have contributed significantly to maintaining elevated pore pressures (Fig. 4; Hendron and Patton, 1985).

In contrast, doubt remains as to the conditions of the failure plane before collapse, to the mechanism that favoured sudden acceleration from decimetres per day to 30 m s^{-1} and to the mechanism controlling rates of movement before catastrophic collapse. Thus, interpretations differ in treating the collapse as the reactivation of a relict landslide (Hendron and Patton, 1985; Pasuto and Soldati, 1991) or as a first-time movement (Skempton, 1966; Petley, 1996; Petley and Allison, 1997), while the rapid onset of catastrophic movement has been attributed to the frictional heating of pore water (Voight and Faust, 1982; D.L. Anderson in Hendron and Patton, 1985; Nonveiller, 1992) or to a decrease in clay shear strength with increasing strain rate (Tika and Hutchinson, 1999). As regards to precollapse accelerations, Voight (1988) observed that
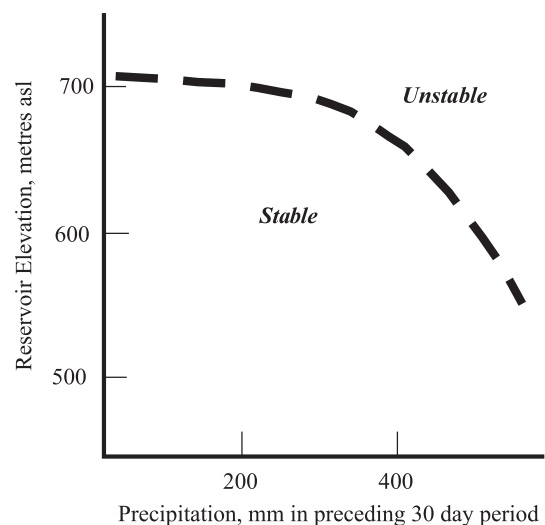

Fig. 4. The effect of water accumulation on slope stability at Mt. Toc. In combination, the reservoir level and precipitation must exceed a critical threshold (dashed curve) to render the slope unstable. Similar trends (but with different threshold values) are seen when considering precipitation over the preceding 7-, 15- and 45-day periods. After Hendron and Patton (1985).

for 2 months before catastrophic failure, the inverse rates of slope movement decreased linearly with time and qualitatively linked such behaviour to rock fracturing. Voight's observations have since been shown to be consistent with the failure behaviour of clay at high pressure (Petley and Allison, 1997; Petley, 1999) and a new model of slow cracking (McGuire and Kilburn, 1997; Kilburn and Voight, 1998). Applied to Mt. Toc, the interpretation has been considered problematic since it implies brittle failure within the clay. However, as described below, recent experiments indicate that clay can indeed behave as a brittle material under the loads expected for deep-seated slope failure.

4. Brittle failure in clay

Although clay is rarely considered to be a brittle material, recent experimental studies (Burland, 1990; Horseman et al., 1993; Taylor and Coop, 1993; Petley, 1995) have shown that brittle behaviour can indeed occur in undisturbed clay samples under loads of $1-10$ MPa, corresponding to depths of the order of 10^2 m. Under such loads (Petley, 1999), clay shows a three-stage approach to failure, analogous to that seen among stronger, brittle rocks (Jaeger, 1969; Hallbauer et al., 1973). Best illustrated on a stress–strain diagram (Fig. 5), the three stages are (1) an elastic deformation for applied shear stresses smaller than a peak value τ_P, (2) continuous creep at τ_P and (3) beyond a critical strain, an abrupt decrease in shear resistance to a residual value τ_R. This behaviour is consistent with microscopic cracking (Jaeger, 1969; Hallbauer et al., 1973; Main and Meredith, 1991; Lockner, 1995; Petley, 1999). Initial elastic deformation involves the stretching of molecular bonds and frictional sliding between the surfaces of any existing small cracks. New cracks appear as the peak stress is approached and continue to open and grow at τ_P until they link together to form a major plane of failure. The shear resistance abruptly decreases to a residual value determined by sliding friction along the new failure plane.

For undrained clay at applied loads of $1-10$ MPa, detailed morphological analyses of the failure surfaces (Petley, 1995, 1999) reveal tear structures at scales of $0.01-0.1$ mm. Peak shear strengths are $\sim 1-2$ MPa and $\tau_P - \tau_R$ is $\sim 0.1-1.0$ MPa (Petley,

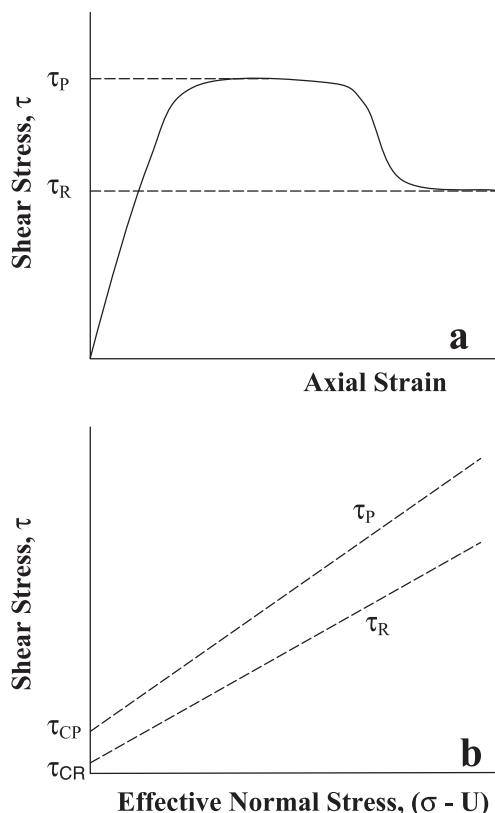Fig. 5. (a) Idealised deformation of rock under loads of $1-10$ MPa. The rock initially deforms elastically for applied stresses smaller than τ_P. It continues to deform at τ_P as microcracks nucleate and grow. When the cracks link to form a major failure plane, the shear resistance of the rock rapidly decreases to τ_R, the stress at which final collapse takes place. Conventional stress–strain diagrams plot deviatoric stress in place of shear stress, but the deformation curves remain qualitatively similar in both cases. (b) Navier–Coulomb failure envelopes for rocks with peak and residual shear resistance. At any given $(\sigma - U)$, microcracking will commence when shear stresses reach the τ_P envelope. At failure, the shear resistance drops to τ_R. The stress difference $\tau_P - \tau_R$ provides the necessary force for sudden slope collapse.

1999); the corresponding values for crystalline rock are τ_P, $\sim 10-50$ MPa, and $\tau_P - \tau_R$, $\sim 0.3-10$ MPa (Jaeger, 1969; Hanks, 1977). Key implications for deep-seated movements are that (1) even for deformation within clay layers, rates of slope movement are controlled by microscopic cracking, and (2) when a major failure plane is developed, the abrupt decrease in shear resistance may provide a force imbalance sufficiently large to trigger catastrophic slope movement.

5. Rates of cracking and slope movement

Applied to deep-seated landslides, slow cracking is an appealing deformation mechanism because it can accelerate under constant applied stress (τ_P in Fig. 5). With the layer being deformed, stresses are concentrated around tiny material flaws (crack nuclei) and at the tips of existing small cracks. When the applied stress exceeds a critical value (dependent on the material's physical properties), the locally concentrated stresses become large enough to break molecular bonds. As each bond breaks, its neighbours relax and release elastic strain energy for driving additional cracking (Lawn, 1993). Unless halted by a reduction of the applied stress, cracks grow at an accelerating rate until they coalesce into a major plane of failure (Main and Meredith, 1991; Lockner, 1995; Kilburn and Voight, 1998).

A second notable feature of slow cracking is that it is readily enhanced by circulating water, which chemically attacks molecular bonds, especially at crack tips (Anderson and Grew, 1977; Atkinson, 1984). Water accumulation within a rock can thus be doubly effective in triggering deep-seated failure. By raising pore pressures, it can first reduce a rock's shear resistance and so effectively introduce a net applied stress (the difference between gravitational stress and rock shear strength). Second, it catalyses microcracking and hence, failure of the stressed layer.

Microcracking is dominated initially by the formation of new cracks, but later by the growth of cracks until a major failure plane is formed (McGuire and Kilburn, 1997; Kilburn and Voight, 1998). While rates of crack nucleation increase exponentially with time (Main and Meredith, 1991), rates of crack growth increase exponentially with crack length (Main et al., 1993). In addition to single cracks, exponential relations also hold for a population of cracks with a fractal size–frequency distribution, using mean values of nucleation rate, growth rate and crack length (Main and Meredith, 1991; Main et al., 1993). Since small cracks must interlink before producing a new plane of failure, it is the onset of deformation dominated by crack growth that provides the essential precursor to slope collapse.

In the case of unstable slopes, cracking occurs due to the downslope stress acting on the deforming horizon. The opening and growth of a population of cracks will thus be recorded macroscopically by a combination of bulk dilation and of downslope displacement. Assuming that each crack event breaks a fixed distance of unbroken rock (whether by nucleating or extending a crack), the rate of cracking becomes equivalent to the number of crack events per unit time. Assuming also that the bulk movements are proportional to the total rate of cracking, rates of downslope displacement (dx/dt) shortly before collapse will be given by (Kilburn and Voight, 1998)

$$dx/dt = (dx/dt)_0 \, e^{\psi(x-x_0)} \qquad (1)$$

where the suffix 0 denotes conditions when crack growth first dominates crack nucleation, and ψ is an inverse length scale that depends on the applied stress, rock properties and the geometry of the crack array. The term $\psi = B\omega^2 S^2 \varphi(dN/dx)/YkT$, where ω is an atomic stretching distance for breaking bonds at crack tips, S is the remote applied stress (due to the downslope weight component of the unstable slope), φ is the mean distance a crack extends during each step-like crack event, Y is Young's modulus, k is Boltzmann's constant, T is the rock's absolute temperature, B is a dimensionless term incorporating Poisson's ratio for the deforming rock, the coefficient of friction along a crack's touching surfaces, and terms describing the geometry of the crack array (Lockner, 1993) and dN/dx denote the number of crack events per unit macroscopic displacement.

Manipulation shows that Eq. (1) is equivalent to a linear decrease with time in the *inverse* rate of displacement,

$$(dx/dt)^{-1} = (dx/dt)_0^{-1} - \psi(t - t_0). \qquad (2)$$

Equating the time of failure with the condition that $(dx/dt)^{-1}$ becomes zero (i.e., rates of deformation become infinitely large), Eq. (2) can be used to forecast the onset of catastrophic collapse by linearly extrapolating measured inverse-rate trends to the time axis at $(dx/dt)^{-1} = 0$. Note also that Eq. (2) describes rates of deformation that increase more quickly than the exponential time increase expected from crack

nucleation. Indeed, an inverse rate–time plot for crack nucleation (for which $(dx/dt)^{-1} \propto e^{-t}$) would yield a curve with negative gradient that approaches $(dx/dt)^{-1} = 0$ asymptotically. In the slow-cracking model, a linear inverse-rate trend with time is diagnostic of movement dominated by crack growth and the approach to major failure.

Final failure at Mt. Toc occurred after more than 2 months of slowly accelerating slope movement. During this interval, the landslide moved about 1–2 m downslope at rates accelerating from about 5 mm to more than 20 cm day^{-1} (Müller, 1964). When the inverse deformation rate during this interval is plotted against time (Fig. 6), a clearly linear decrease is observed, as expected from the slow-cracking model (Eq. (2)). This is the same trend found empirically by Voight (1988). The key feature here is that the slow-cracking model provides a physical basis for using such trends to quantify the approach to catastrophic collapse. Indeed, in the case of Mt. Toc, an inverse linear trend for the final precollapse acceleration is evident by the beginning of September (day 30 in Fig. 6) so that, had the model been available at that time, catastrophic failure might have been forecasted almost a month before it occurred.
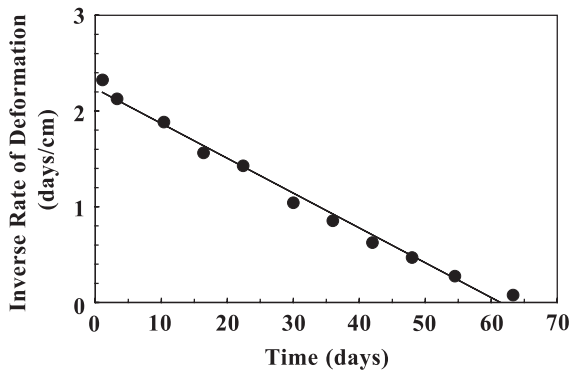

Fig. 6. Inverse rates of horizontal slope movement before the catastrophic collapse of Mt. Toc into the Vajont reservoir on 9 October 1963 (see also Fig. 3). The inverse-deformation rate decreases linearly with time as expected from slow cracking dominated by crack growth. Linear regression gives an R^2 correlation coefficient of 0.99. A linear trend would have been apparent at least by day 30, yielding a 30-day forecast for major collapse. Errors on measured rates are estimated to have been less than 5%, within the size of the circles. Data from Müller (1964) and Voight (1988).

6. Slow cracking and seismicity before collapse

The slow-cracking model assumes that mean rates of precollapse movement are proportional to rates of cracking. Since cracking triggers seismic events, it is expected that accelerating rates of seismicity should also accompany the accelerating displacements. No such relation can be seen between the seismicity and movements recorded in the 2 months preceding Mt. Toc's catastrophic failure. However, indirect evidence suggests that movement was controlled by low-level seismicity below the recording threshold of the monitoring system.

Precollapse seismicity at Mt. Toc was monitored by a single seismometer alongside the top of the Vajont dam (Caloi, 1966; Belloni and Stefani, 1992). Between May 1960 and October 1963, about 50 events were recorded, of which four events had Richter Magnitudes in the range 0–0.5, while the remainder had magnitudes between 0 and −2 (the minimum value corresponding to a threshold seismic amplitude of about 1 μm is due to an event 1 km from the seismometer). Most of the events had epicentres across the unstable slope. However, their depths could be located only crudely, given the operation of just one seismometer. Events below the monitoring station occurred at depths between about 200 m (close to the level of the future failure plane) and 800 m. Events across the moving mass occurred at undetermined positions above the 725.6 m altitude of the seismometer (Belloni and Stefani, 1992). None of the recorded events, therefore, can confidently be placed along the future plane of failure and may in fact have represented a general cracking throughout the unstable slope (Fig. 2).

In addition, during the final acceleration from August to October 1963, two seismic events were recorded in August, 15 events were registered in the first 3 weeks of September and none at all were monitored between the last week of September and October collapse (Fig. 3; Belloni and Stefani, 1992). Such a seismic pattern is clearly not that expected from accelerating slope movement caused by accelerating rates of cracking. This apparent contradiction can be resolved if crack events along the deforming clay horizons had been too small to be detected.

Experiments simulating clay deformation at loads appropriate to the Mt. Toc failure suggest that tearing

occurs at scales of $10^{-5} - 10^{-4}$ m (Petley and Allison, 1997). Assuming that bulk slope movement is controlled by a large number of discrete crack events across the whole surface of the deforming horizon, then each bulk displacement by an amount x will be associated with a seismic moment M_0 of

$$M_0 = G A x \qquad (3)$$

where G and A are the rigidity and surface area of the cracking layer. Seismic moment in turn can be related to seismic magnitude m by (Kanamori and Anderson, 1975; Hanks and Kanamori, 1979)

$$\log M_0 = cm + d \qquad (4)$$

where c measures fracture geometry and has a value of 1.5, and empirical studies yield $d = 9.1$ for M_0 in joules.

For undrained clay at loads of $1-10$ MPa, $G \sim 10^8$ Pa (Petley, 1999). Setting the Vajont slide area to its maximum possible value of 2×10^6 m^2 and x between the limits 10^{-5} and 10^{-4} m, Eqs. (3) and (4) yield maximum magnitudes of between 0 and 1 per incremental bulk displacement. Such magnitudes would have been well within the recording range of the Vajont seismometer. However, the estimated magnitudes are based on earthquakes far enough from a seismometer to be registered as a single event. At Vajont, recordings were being made at $\sim 0.1-1$ km from the failure plane. Under such conditions, bulk movement across the whole surface of the failure plane would not be recorded as a single event but as a number of much smaller events, each one affecting an area orders of magnitude less than that of the entire failure plane.

To a first approximation, a displacement x during a single seismic event can be related to an area of failure of about $6(G/\Delta\tau)^2 x^2$ (assuming a circular area; Scholz, 1990), where $\Delta\tau$ is the drop in shear stress across the crack surface caused by relaxation of the stretched molecular bonds in the adjacent rock. For very small crack events, $\Delta\tau$ is nominally about 1% of the applied shear stress (Spottiswoode and McGarr, 1975; Scholz, 1990). At Mt. Toc, a notional value for $\Delta\tau$ is $\sim 10^4$ Pa, yielding an area of failure $A_f \sim 6 \times 10^8 x^2$. The landslide can thus be imagined to have moved by a collection of tearing events across adjacent areas of size A_f. As an area A_f tears, stresses become concentrated in neighbouring rock until tearing occurs across adjacent areas also of A_f. Note that A_f only represents the area in which a collection of small tears appears at about the same time and does not necessarily indicate the dimensions of an uninterrupted discontinuity.

Taking the previous limits of x ($10^{-5} - 10^{-4}$ m), the magnitudes associated with displacements over areas of A_f are between -3 and -5 below the recording threshold of the Vajont seismometer. The recorded seismicity, therefore, could not have measured rates of cracking within the clay horizon that ultimately failed, but was instead linked to sporadic cracking in locally weak volumes throughout the entire unstable mass. In other words, the recorded seismicity was not a reliable measure of the approach to catastrophic slope failure.

7. Slow cracking as a control on collapse volume and acceleration

Just before the onset of deformation, the gravitational driving stress τ_g is balanced by the peak resistance τ_P of material in the deforming layer (incorporating adjustments due to the pore pressures of contained fluids). Using the infinite-slope approximation for simplicity, $\tau_g \sim \rho g h \sin\alpha$ (where α is the mean angle of slope failure). Setting $h = CV^{1/3}$, the volume V of the unstable slope is $\sim [\tau_P/(\rho g C \sin\alpha)]^3$. Typical ranges for α and C are $20-40°$ and $0.1-0.5$ (Kilburn and Sørensen, 1998). For $\tau_P \sim 1-2$ MPa, these values yield minimum volumes and depths at failure of about $5-10$ million m^3 and $\sim 10^2$ m, both of which agree well with field data (Hsü, 1975; Melosh, 1987).

When τ_g exceeds rock resistance τ_r, an unstable mass moves downslope with an acceleration a given by (Hoek and Bray, 1997)

$$a = (\tau_g - \tau_r)/\rho h \qquad (5)$$

where ρ and h are the mean density and thickness of the moving mass.

Early deformation is dominated by the appearance of new, but isolated cracks, during which period material resistance decreases by only a small

amount below its peak value. Initial slope movements thus accelerate very slowly. In contrast, when growing cracks finally link to form a major plane of failure, τ_r abruptly decreases to its residual value τ_R. Since the gravitational stress remains unchanged at τ_P, the sudden drop in resisting stress can provide the force imbalance for catastrophic acceleration.

To a first approximation, the difference between peak and residual strength $(\tau_P - \tau_R) \approx \gamma \tau_P$. Setting $\tau_P = \tau_g = \rho g h \sin\alpha$, Eq. (5) yields $a \approx \gamma g \sin\alpha$. Taking clay as the most probable weak material in a crustal sequence, γ is about $0.1-0.2$ (Hendron and Patton, 1985; Petley, 1999), for which catastrophic accelerations are expected to be between $0.4-0.8$ and $0.6-1.2$ m s^{-2} for angles of slope failure between $25°$ and $40°$.

From the Coulomb–Mohr failure criterion, τ_r along the future plane of failure is given by $\tau_r = \tau_c + \mu[1 - (U/\sigma)]\sigma$, for which τ_c is material cohesion, μ is the coefficient of sliding friction and $[1 - (U/\sigma)]\sigma$, the effective normal stress, is the difference between actual normal pressure σ and fluid pore pressure U; for failure slopes with mean angle α, $\sigma \sim \rho g h \cos\alpha$.

Expanding for τ_R in Eq. (5), the friction coefficient can be expressed as

$$\mu = [1 - (\gamma \sin\alpha)][1 - (U/\sigma)]^{-1}\tan\alpha \qquad (6)$$

assuming that cohesion is negligible.

Applied to Mt. Toc, $U/\sigma \approx 0.3$ (Voight and Faust, 1982) and $\alpha \approx 20°$. Given that $\gamma = 0.1-0.2$, the collapse acceleration is expected to have been $0.35-0.70$ m s^{-2}, which, for a total mass displacement s of about 500 m, yields an estimated collapse time $(\sim (2s/a)^{1/2})$ of $40-60$ s, compared with field estimates of about 45 s (Voight and Faust, 1982; Hendron and Patton, 1985). Eq. (6) further indicates a friction coefficient of about 0.5 for the deforming clay layer, consistent with the range $0.4-0.5$ found for undrained clays deforming at loads of $1-10$ MPa (Petley, 1999). Importantly, the essential dynamic features of the Mt. Toc collapse can be explained in terms of ordinary chemical and mechanical rock properties without recourse to special mechanisms, such as the vaporization of water, for reducing rock friction.

8. Discussion

Slow rock cracking is commonplace in the Earth's crust and has been identified as an important precursor to major earthquakes (Main, 1999) and volcanic eruptions (McGuire and Kilburn, 1997; Kilburn and Voight, 1998). It is not surprising, therefore, that slow failure may also precede giant and catastrophic slope collapse.

The model presented here interprets precollapse movements in terms of the nucleation, growth and coalescence of a fractal population of cracks. Initial deformation is assumed to be controlled by the opening of new but isolated cracks. Subsequent deformation occurs more rapidly as crack growth dominates crack nucleation. Eventually, clusters of small cracks join together to form larger fractures, and these in turn link together to create a plane of failure. An abrupt drop in shear resistance, following formation of the failure plane, provides the force imbalance necessary to drive catastrophic collapse.

The drop in shear resistance upon fracturing tends to increase with a rock's peak shear strength. Such failure under gravity cannot occur at shallow depths since the applied stresses are smaller than the peak resistances of continuous rock. Shallow landslides are thus associated (1) with the movement of loose material, such as soil or of chemically weakened or previously fractured rock, and (2) with very small stress drops for which initial accelerations are too small to trigger catastrophic movements. In other words, the rapid accelerations required for catastrophic collapse can only be achieved by fracturing rock with a large difference between peak and residual strength, and hence, also a large peak strength. As a result, such collapse requires depths of failure large enough to induce brittle deformation, and these in turn are associated with unstable volumes greater than a threshold value.

While brittle failure and associated stress drops can account for the accelerations and minimum volumes associated with sturzstroms, rates of preceding slow cracking can also explain observed accelerations in slope movement before collapse. When deformation is dominated by crack nucleation, bulk movement accelerates exponentially with time. Such movements are not intrinsically dangerous since the new cracks remain isolated. However, when crack growth domi-

nates, bulk movements accelerate more rapidly at a rate whose inverse happens to decrease linearly with time. Extrapolations of the linear inverse-rate trend offer the prospect of forecasting catastrophic failure.

In the case of Mt. Toc's collapse in 1963, a linear inverse-rate trend was evident at least a month before the October catastrophe. Previous analyses of the event have focussed on the destabilising effect of increased pore pressure due to filling of the reservoir. Hendron and Patton (1985), in particular, argued that both reservoir filling and cumulative rainfall were crucial to triggering slope movements. The current analysis is entirely consistent with these earlier investigations. Thus, by reducing the effective normal pressure, water pore pressure reduced the peak strength of, in Mt. Toc's case, clay horizons at depths of $100-200$ m, until existing gravitational shear stresses were able to initiate movement. At loads of ~ 1 MPa, the deep clay deformed in a slow brittle manner until, on 9 October 1963, the growing cracks combined into a single failure plane, abruptly reducing the clay's resistance from its peak to residual values. The resulting force imbalance was sufficiently large to raise slope accelerations to ~ 0.5 m s^{-2}, triggering a collapse that was complete within about 45 s.

At that time, the high speed of the 1963 collapse was completely unexpected. Previous increases in slope acceleration (between 1960 and 1963) had been restricted by lowering the reservoir level, and maximum daily movements had approached only 4 cm. These subcatastrophic movements are consistent with deformation dominated by crack nucleation without the formation of an extensive plane of failure. By reducing pore pressures, lowering the reservoir level had been able to decrease the imposed stress imbalance sufficiently to inhibit further crack nucleation. However, by September 1963, the cumulative strain in the basal clay was large enough for deformation to enter the stage dominated by crack growth. On this occasion, bulk deformation was already accelerating too rapidly to be slowed significantly by lowering the reservoir level. If correct, this interpretation would expect slope movements before September 1963 to have increased only exponentially with time in accordance with pervasive crack nucleation. Exponential time increases in velocity were indeed recorded on at least one occasion, during the month preceding the small toe collapse on 4 November 1960

(Voight, 1988). This circumstance appears to contradict the slow-cracking model, until account is taken of the fact that the deformation records for this period refer to movements beyond the small region of the toe that collapsed, and so would not have recorded faster local accelerations within the toe itself (Figs. 1 and 2). Further studies are continuing for the 1960–1963 sequence of movements.

Mt. Toc's rapid collapse has also generated numerous investigations into conditions for rapidly reducing rock friction during sliding. By far, the most popular has been the vaporization of groundwater leading to unusually large pore pressures in the sliding layer (Voight and Faust, 1982; D.L. Anderson in Hendron and Patton, 1985; Nonveiller, 1992). These analyses had no data concerning stress drops during clay failure and, to account for large collapse accelerations, were obliged to seek external mechanisms for reducing rock friction. More recent deformation experiments on clays at loads of $\sim 1-10$ MPa (Petley, 1999), relevant to conditions along Mt. Toc's failure horizon (Hendron and Patton, 1985), offer the alternative explanation that collapse accelerations are controlled by the drop in stress resistance upon clay failure. This extra interpretation does not preclude the possibility of friction reduced by vaporization. However, it does render vaporization a nonessential mechanism and would allow for catastrophic slope collapses in environments (especially extraterrestrial settings) within which pore fluids may not have been readily available.

The Mt. Toc example also suggests that, at least in clay, microcracking is associated with seismic events that may be too small to be recorded by conventional seismometers, in part because the events are small, and in part because they occur at levels deep enough for their signals to be strongly attenuated before reaching the surface. Thus, as a measure of rates of microcracking, bulk movements are considered to be more reliable than detected seismicity, which might instead reflect sporadic cracking in weak zones located away from the failure plane.

9. Conclusions

Giant and catastrophic slope collapse is a natural result of accelerating deformation due to slow rock

cracking. The model presented here suggests that inverse rates of deformation decreasing linearly with time are diagnostic of the approach to bulk failure and collapse. Although such a trend has been described on empirical grounds (Voight, 1988), the slow-cracking model provides a physical basis for developing quantitative forecasts of slope collapse.

Combined with rapid decreases from peak to residual strength in the rock undergoing failure, the slow-cracking model also accounts for the minimum volumes required for catastrophic collapse and the emplacement of sturzstroms, as well as the typical accelerations inferred for such collapse. Moreover, slow cracking is readily catalysed by circulating water and so offers a natural mechanism for explaining the catastrophic failure of deep-seated landslides initially rendered unstable by internal accumulation of water and the resultant increase in pore pressure.

Acknowledgements

References

Anderson, O.L., Grew, P.C., 1977. Stress corrosion theory of crack propagation with applications to geophysics. Rev. Geophys. Space Sci. 15, 77–104.

Atkinson, B.K., 1984. Subcritical crack growth in geological materials. J. Geophys. Res. 89, 4077–4114.

Bassett, R.H., 1978. Time-dependent strains and creep in rock and soil structures. In: Pomeroy, C.D. (Ed.), Creep of Engineering Materials. Inst. Mech. Eng., London, pp. 11–38.

Belloni, L.G., Stefani, R.F., 1992. Natural and induced seismicity at the Vajont slide. In: Semenza, E., Melidoro, G. (Eds.), Proc. Meeting 1963 Vaiont Landslide, Ferrara 1986. Univ. of Ferrara, Ferrara, pp. 115–132.

Blodgett, T.A., Blizard, C., Isacks, B.L., 1998. Andean landslide hazards. In: Kalvoda, J., Rosenfeld, C.L. (Eds.), Geomorphological Hazards in High Mountain Areas. Kluwer Academic Publishing, Dordrecht, pp. 211–227.

Burland, J.B., 1990. On the compressibility and shear strength of natural clays. Geotechnique 40, 329–378.

Caloi, P., 1966. L'Evento del Vajont nei suoi aspetti geodinamici. Istituto Nazionale di Geofisica, Rome.

Hadley, J.B., 1978. Madison Canyon rockslide, Montana, U.S.A. In: Voight, B. (Ed.), Rockslides and Avalanches. Natural Phenomena, vol. 1. Elsevier, Amsterdam, pp. 167–180.

Hallbauer, D.K., Wager, H., Cook, N.G.W., 1973. Some observations concerning the microscopic and mechanical behaviour of quartzite specimens in stiff, triaxial compression tests. Int. J. Rock Mech. Min. Sci. 10, 713–726.

Hanks, T.C., 1977. Earthquake stress-drops, ambient tectonic stresses, and stresses that drive plates. Pure Appl. Geophys. 115, 441–458.

Hanks, T.C., Kanamori, H., 1979. A moment–magnitude scale. J. Geophys. Res. 84, 2348–2352.

Hendron, A.J., Patton, F.D., 1985. The Vaiont slide, a geotechnical analysis based on new geologic observations of the failure surface. US Army Corps of Engineers Technical Report GL-85-5 (2 volumes).

Hoek, E., Bray, J.W., 1997. Rock Slope Engineering, 3rd ed. IMM and E&FN Spon, London. Revised.

Horseman, S.T., Winter, M.G., Entwistle, D.C., 1993. Triaxial experiments on Boom Clay. In: Cripps, J.C., Coulthard, J.M., Culshaw, M.G., Forster, A., Hencher, S.R., Moon, C.F. (Eds.), The Engineering Geology of Weak Rock. Balkema, Rotterdam, pp. 35–44.

Howard, K.E., 1973. Avalanche mode of motion, implication from lunar examples. Science 180, 1052–1055.

Hsü, K.J., 1975. On sturzstroms—catastrophic debris streams generated by rockfalls. Geol. Soc. Amer. Bull. 86, 129–140.

Jaeger, J.C., 1969. Elasticity, Fracture and Flow, 3rd ed. Chapman & Hall, London.

Kanamori, H., Anderson, D.L., 1975. Theoretical basis of some empirical relations in seismology. Bull. Seismol. Soc. Am. 65, 1073–1095.

Kilburn, C.R.J., Sørensen, S.-A., 1998. Runout lengths of sturzstroms: the control of initial conditions and of fragment dynamics. J. Geophys. Res. 103, 17877–17884.

Kilburn, C.R.J., Voight, B., 1998. Slow rock fracture as eruption precursor at Soufriere Hills volcano. Montserrat. Geophys. Res. Lett. 25, 3665–3668.

Lawn, B., 1993. Fracture of Brittle Solids, 2nd ed. Cambridge Univ. Press, Cambridge.

Lockner, D.A., 1993. Room temperature creep in saturated granite. J. Geophys. Res. 98, 475–487.

Lockner, D.A., 1995. Rock failure. In: Ahrens, T.J. (Ed.), Rock Physics and Phase Relations. A Handbook of Physical Constants. AGU Reference Shelf, vol. 3. AGU, Washington, DC, pp. 127–147.

Lopes, R.M.C., Guest, J.E., Hiller, K., Neukum, G., 1982. Further evidence for a mass movement origin of the Olympus Mons aureole. J. Geophys. Res. 87, 9917–9928.

Main, I.G., 1999. Applicability of time-to-failure analysis to accelerated strain before earthquakes and volcanic eruptions. Geophys. J. Int. 139, F1–F6.

Main, I.G., Meredith, P.G., 1991. Stress corrosion constitutive laws as a possible mechanism of intermediate-term and short-term seismic event rates and b-values. Geophys. J. Int. 107, 363–372.

Main, I.G., Sammonds, P.R., Meredith, P.G., 1993. Application of a modified Griffith criterion to the evolution of fractal damage during compressional rock failure. Geophys. J. Int. 115, 367–380.

Mantovani, F., Bollettinari, G., Ghirelli, C., 1991. The Vaiont rock landslide. In: Panizza, M., Soldati, M., Coltellacci, M.M. (Eds.), European Experimental Course on Applied Geomorphology: 2. Proceedings, Ist. Geol. Univ. Modena. Univ. of Modena, Modena, pp. 65–76.

McGuire, W.J., Kilburn, C.R.J., 1997. Forecasting volcanic events: some contemporary issues. Geol. Rundsch. 86, 439–445.

McSaveney, M.J., 1978. Sherman glacier rock avalanche, Alaska, U.S.A. In: Voight, B. (Ed.), Rockslides and Avalanches: 1. Natural Phenomena. Elsevier, Amsterdam, pp. 197–258.

Melidoro, G., 1992. Introductory report. In: Semenza, E., Melidoro, G. (Eds.), Proc. Meeting 1963 Vaiont Landslide, Ferrara 1986. Univ. of Ferrara, Ferrara, pp. 31–42.

Melosh, H.J., 1987. The mechanics of large rock avalanches. Rev. Eng. Geol. VII, 41–49.

Müller, L., 1964. The rock slide in the Vaiont valley. Felsmech. Ingenieurgeol. 2, 148–212.

Nonveiller, E., 1992. Vaiont slide: influence of frictional heat on slip velocity. In: Semenza, E., Melidoro, G. (Eds.), Proc. Meeting 1963 Vaiont Landslide, Ferrara 1986. Univ. of Ferrara, Ferrara, pp. 187–197.

Pasuto, M., Soldati, A., 1991. Some cases of deep-seated gravitational deformations in the area of Cortina d'Ampezzo (Dolomites). Proceedings of European Short Course on Applied Geomorphology, vol. 2. Univ. of Modena, Modena, pp. 91–104.

Petley, D.N., 1995. The deformation of mudrocks. PhD thesis, University of London.

Petley, D.N., 1996. The mechanics and landforms of deep-seated landslides. In: Brooks, S., Anderson, M. (Eds.), Advances in Hillslope Processes. Wiley, Chichester, pp. 823–835.

Petley, D.N., 1999. Failure envelopes of mudrocks at high effective stresses. In: Aplin, A.C., Fleet, A.J., Macquaker, J.H.S. (Eds.), Physical Properties of Muds and Mudstones. Spec. Publ. - Geol. Soc. Lond., vol. 158. Geol. Soc. London, London, pp. 61–71.

Petley, D.N., Allison, R.J., 1997. The mechanics of deep-seated landslides. Earth Surf. Processes Landf. 22, 747–758.

Plafker, G., Ericksen, G.E., 1978. Nevados Husacarán avalanches, Peru. In: Voight, B. (Ed.), Rockslides and Avalanches: 1. Natural Phenomena. Elsevier, Amsterdam, pp. 277–314.

Scholz, C.H., 1990. The Mechanics of Earthquakes and Faulting. Cambridge Univ. Press, Cambridge.

Semenza, E., 1965. Sintesi degli studi geologici sulla frana del Vaiont dal 1959 al 1964. Mem. Mus. Trident. Sci. Nat., A XXIX–XXX (16), 1–51 (English translation in Hendron and Patton, 1985).

Semenza, E., Sapigni, M., 1986. Carta e profili geologici della Valle del Vaiont e zone limitrofe. In: Semenza, E., Melidoro, G. (Eds.), Proc. Meeting 1963 Vaiont Landslide, Ferrara 1986. Univ. of Ferrara, Ferrara.

Semenza, E., Melidoro, G. (Eds.), 1992. Proc. Meeting 1963 Vaiont Landslide, Ferrara 1986. Univ. of Ferrara, Ferrara.

Skempton, A.W., 1966. Some observations on tectonic shear zones. Proc. First. Int. Conf. Rock Merchanics, Lisbon, vol. 1, pp. 551–552.

Spottiswoode, S.M., McGarr, A., 1975. Source parameters of tremors in a deep-level gold mine. Bull. Seismol. Soc. Am. 65, 93–112.

Taylor, R.N., Coop, M.R., 1993. Stress path testing of Boom Clay from Mol, Belgium. In: Cripps, J.C., Coulthard, J.M., Culshaw, M.G., Forster, A., Hencher, S.R., Moon, C.F. (Eds.), The Engineering Geology of Weak Rock. Balkema, Rotterdam, pp. 77–82.

Ter-Stepanian, G., 1966. Types of depth creep of slopes in rock masses. Proc. First Congress Int. Soc. Rock Mechanics, Lisbon, vol. 2, pp. 157–160.

Tika, Th.E., Hutchinson, J.N., 1999. Ring shear tests on soil from the Vaiont landslide slip surface. Geotechnique 49, 59–74.

Voight, B., 1978. Rockslides and Avalanches: 1. Natural Phenomena. Elsevier, Amsterdam.

Voight, B. (Ed.), 1988. A Method for Prediction of Volcanic Eruptions. Nature 332, 125–130.

Voight, B., Faust, C., 1982. Frictional heat and strength loss in some rapid landslides. Geotechnique 32, 43–54.